

# Progressive Failure Analysis of Shuttle Reinforced Carbon-Carbon Plate Specimens

Vladimir S. Sokolinsky\* and Jerry Housner†

Jonas Surdenas‡

and

Frank Abdi§

Alpha STAR Corporation, Long Beach, CA, 90804

A progressive failure analysis of two reinforced carbon-carbon plate specimens subject to three-point bending was carried out under contract to NASA by the Alpha STAR Corporation. The GENOA computer code was used to analyze both one and one-and-a-half inch long composite plate specimens. The failure propagation analysis revealed deep qualitative differences in the behavior of the short (one inch long) and long (one-and-a-half inch long) specimens. In the short plate, primary and secondary delaminations were predicted, progressive delamination being the cause of premature failure of the plate, whereas practically no delamination was predicted in the long specimen. The final failure at mid-span was predicted in both the short and long specimens. The predicted failure loads and damage mechanisms were in excellent agreement with the experiments.

## Nomenclature

$S_{11\alpha}, S_{11\beta}$	=	ply tensile or compressive strength in longitudinal direction
$S_{22\beta}, S_{22\beta}$	=	ply tensile or compressive strength in transverse direction
$S_{12S}$	=	ply shear strength
$\sigma_{11\alpha}, \sigma_{11\beta}$	=	ply tensile or compressive stress in longitudinal direction
$\sigma_{22\beta}, \sigma_{22\beta}$	=	ply tensile or compressive stress in transverse direction
$\sigma_{12S}$	=	ply shear stress
$E_{11}$	=	ply Young's modulus in longitudinal direction
$E_{22}$	=	ply Young's modulus in transverse direction
$\nu_{12}, \text{etc.}$	=	ply Poisson's ratio
$K_{12\alpha\beta}$	=	ply theory-experiment in-plane shear correlation factor

## I. Introduction

ON February 1, 2003 the Columbia Shuttle STS-107 burnt up during re-entry to Earth. The Columbia Accident Investigation Board concluded that the loss of the vehicle and crew was caused by failure of the reinforced carbon-carbon (RCC) leading edge of the left wing of the Shuttle on re-entry. The progressive failure process apparently started at the location on the leading edge that was impacted by the foam pieces separated from the external tank during lift off. Because RCC provides the main line of thermal protection for the wings, its failure allowed hot gases to enter the wing cavity and undermine the strength of the wing supporting structure.

NASA has decided to continue using RCC leading edges on the Shuttle. Therefore much work has been done to significantly improve understanding of the progressive failure process in RCC structures. As one step, NASA

---

\* Structural Scientist, 5199 East Pacific Coast Highway, Suite 410, Member AIAA.

† Consultant, 5199 East Pacific Coast Highway, Suite 410, Member AIAA.

‡ Sr. Structural Scientist, 5199 East Pacific Coast Highway, Suite 410, Member AIAA.

§ CEO, 5199 East Pacific Coast Highway, Suite 410, Member AIAA.

performed an experimental investigation of two RCC composite plate specimens—one and one-and-a-half inch long—subject to three-point bending.

In the present work, the GENOA computer code was used to predict progressive failure mechanisms in the short (one inch long) and long (one-and-a-half inch long) NASA RCC composite plate specimens subject to three-point bending. The primary goal of the numerical simulations was the accurate prediction of the onset of delamination together with the identification and qualitative characterization of the failure mechanisms in the RCC composite plates caused by transverse localized bending loading.

In what follows, the progressive failure analysis procedure implemented in the GENOA computer code is briefly outlined. Then geometrical and mechanical properties of the RCC plate specimens are described, followed by the description of the calibration procedure and finite element models of the specimens. Next, the results of the GENOA progressive failure analysis of the RCC plate specimens are presented, discussed and compared to the NASA experiments.

## II. GENOA Progressive Failure Analysis

The GENOA computer code enhances commercial finite element analysis software, providing tools necessary for advanced numerical analysis of composite materials and structures. It enables analysis and visualization of failure propagation throughout complicated composite structures using as an input macro- or micromechanical composite material properties. The computational methodology of the GENOA progressive failure analysis accounts for the nonlinear response of a composite structure taking into consideration (a) degradation of composite constituents and (b) resulting redistribution of internal stresses and strains. All the internal response fields and accumulated damage at any structural location can be visualized at any point along the nonlinear equilibrium pass of a composite structure. The ability to operate with the micromechanical material input is an important advantage of GENOA because essentially all damage events originate at micro-scale.

The GENOA progressive failure numerical analysis is organized in the following way. The response fields at the structural scale (stress, displacements, etc.) obtained from the commercial finite element solver are transformed to the laminate and lamina scales using classical laminate theory. The majority of conventional finite element composite analyses do not track damage events beyond this level. Using GENOA, damage is tracked down to the unit cell of a composite material and further to micro-scale (fibers and matrix) at the specific finite element node.

Stress-strain fields at the micro-scale are derived from those at the lamina scale using micro-stress theory.<sup>2-5</sup> These micro stress-strain fields are used in the

evaluation of damage state of the composite material based on the failure criteria presented in Fig. 1. When damage is detected according to the criteria of Fig. 1, a set of material degradation rules is applied to the composite structure being analyzed (Refs. 2–5). Accumulation of damage may lead to the fracture at ply level following by the fracture at laminate level at a specific location in the structure. A finite element node is considered to have fractured when all the plies have fractured at that node.

Because damage state is analyzed at the micro-scale, various types of damage (Fig. 1) can be detected at the same location in the structure. Therefore, cracking of composite matrix and breaking of fibers may be observed at the same node of a finite element mesh or the same point on a finite element.

Delamination damage plays an important role in the present analysis. As can be seen from Fig. 1, the presence of delamination in the structure may be indicated by the damage due to excessive normal tensile and out-of-plane shear stresses, and large relative in-plane rotations of the adjacent plies (Ref. 2). As mentioned previously, various types of damage can be detected at the same location in the structure. Therefore, different sources of delamination damage can amplify each other to produce an effect of fast delamination propagation through a composite structure leading to a premature failure of the structure.

Finally, a comment on the modified distortion energy criterion is in order. This criterion was suggested by Chamis<sup>6</sup> in the following form

- |                               |                                    |
|-------------------------------|------------------------------------|
| 1. Longitudinal tension       | 9. Strain invariant failure theory |
| 2. Longitudinal compression   | 10. Normal compression             |
| 3. Transverse tension         | 11. User defined criteria          |
| 4. Transverse compression     | 12. Normal tension                 |
| 5. In-plane shear (+)         | 13. Transverse normal shear (+)    |
| 6. In-plane shear (-)         | 14. Transverse normal shear (-)    |
| 7. Fiber strain limit         | 15. Longitudinal normal shear (+)  |
| 8. Modified distortion energy | 16. Longitudinal normal shear (-)  |
|                               | 17. Relative rotation criteria     |
- Delamination Criteria →

**Figure 1. Micro-mechanics failure criteria.**

$$\left(\frac{\sigma_{11\alpha}}{S_{11\alpha}}\right)^2 + \left(\frac{\sigma_{22\beta}}{S_{22\beta}}\right)^2 - K_{12\alpha\beta} \frac{\sigma_{11\alpha}}{S_{11\alpha}} \frac{\sigma_{22\beta}}{S_{22\beta}} + \left(\frac{\sigma_{12S}}{S_{12S}}\right)^2 < 1 \quad (1)$$

where the directional interaction factor is defined as

$$K_{12\alpha\beta} = K'_{12\alpha\beta} \frac{(1 + 4\nu_{12} - \nu_{13})E_{22} + (1 - \nu_{23})E_{11}}{[E_{11}E_{22}(2 + \nu_{12} + \nu_{13})(2 + 4\nu_{21} + \nu_{23})]^{1/2}} \quad (2)$$

### III. Modeling of the RCC Plate Specimens

To investigate the progressive failure process in RCC structures, NASA used two composite plate specimens—short (one inch long) and long (one-and-a-half inch long)—subject to three-point bending (Fig. 2). Both specimens were half-inch wide and were fabricated of nineteen plies of plane-weave RCC material, which added up to a total thickness of 0.229 inch for each specimen. The laminate was constructed in a 0/90 cross-ply pattern with the resultant mechanical properties essentially equivalent in the orthogonal directions. The fiber volume fraction of the RCC composite material was 60 %.

#### A. Material Characterization

The material constituent (fiber and matrix) properties of the RCC material, which are required for the GENOA progressive failure analysis, were obtained through a calibration procedure. This procedure involves an iterative adjustment of the material constituents properties to match the measured composite coupon response. A reliable calibration procedure requires test data obtained from the five basic ASTM coupon tests including uniaxial tension and compression in the longitudinal and transverse directions, and in-plane shear. Generic material data obtained from manufacturer or other reliable sources is used to initiate the calibration procedure.

In the present analysis, the calibration procedure was based on the test data for the RCC coupons given in Ref. 1. The material composite analyzer (MCA) module in GENOA, which calculates lamina and laminate properties given the material constituent properties, was used to perform the automated calibration procedure. The MCA processor uses classical laminate theory taking into consideration the effects of moisture, cure and service temperatures, voids, residual stresses and manufacturing defects. The calibrated fiber and matrix properties are given in Tables 1 and 2. These properties were entered into the GENOA material database, whereas the composite lay-up of the RCC specimens was described in the ply schedules part of the GENOA input file.

A flexible ply schedules format used in GENOA conveniently describes virtually any composite lay-up with proper accounting for the constitutive properties, cure and service temperatures, and moisture content of each ply.

#### B. Modeling Assumptions

The following assumptions were used in the present study as the basis for the progressive failure analysis of the RCC specimens:

- 1) The influence of the external and internal layers, which are used to protect the RCC material of the leading edge from reacting with oxygen, on the mechanical response of the plates is negligible.

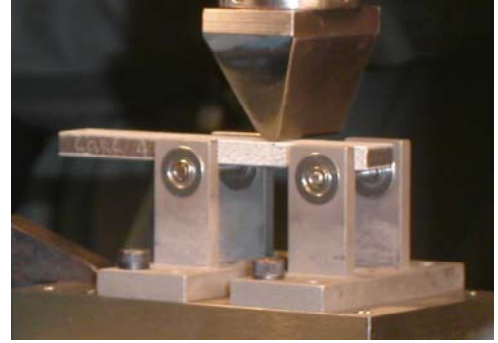


Figure 2. NASA experimental setup.

Table 1 Mechanical properties of the RCC fibers

Property	Value
Longitudinal tensile modulus (11)	2.10E6 psi
Longitudinal compressive modulus (11)	4.50E6 psi
Transverse tensile modulus (22)	2.10E6 psi
Transverse compressive modulus (22)	4.50E6 psi
Shear modulus (12 and 13)	1.00E6 psi
Shear modulus (23)	0.23E6 psi
Poisson's ratio (12)	0.23
Poisson's ratio (23)	0.23
Longitudinal tensile strength	4.00E4 psi
Longitudinal compressive strength	6.00E4 psi
Transverse tensile strength	4.00E4 psi
Transverse compressive strength	6.00E4 psi

- 2) The friction contact conditions at the free supports and loading rig can be closely approximated by pinned-rolling boundary conditions and knife-type loading.
- 3) The experimental loading rate is sufficiently slow to be approximated by static incremental loading.
- 4) The specimens are free of any preloading stresses-strain conditions.

The finite element meshes of the short and long specimens consisted of 200 and 300 Mindling-Reissner shell elements, respectively. Displacement control path-following procedure was used to compute the equilibrium path to failure of the RCC plate specimens. Please note that GENOA accounts for both the in-plane and out-of-plane strength and stiffness contributions of the woven fabric material, which is especially important for the present analysis.

#### IV. Results and Discussion

In this section, the GENOA progressive failure analysis of the short and long RCC plate specimens is presented.

##### A. Short Plate Specimen

A comparison between the predicted and measured load-displacement response of the short RCC plate specimen subject to three-point bending is shown in Fig. 3. Points A through F on the predicted load-displacement curve indicate the onset of various types of damage in the specimen with increasing external load. At point A (~125 pounds), transverse matrix micro-cracking initiates at the bottom ply of the specimen. The process of matrix micro-cracking in the lower plies intensifies between the points A and B, and transverse compressive damage initiates in the top ply at a 270 pound load level. Also, at point B, the modified distortion energy criterion in Eq. 1 is violated. When the applied load reaches 280 pounds, delamination failures begin to develop. The presence of delaminations is first indicated by the large relative in-plane rotations of the adjacent second, third and fourth plies from the bottom. This is a secondary delamination, which grows relatively slowly towards the center of the specimen. A primary delamination initiates between the plies close to the middle plane of the specimen at 300 pounds (point D). It quickly propagates from the center of the specimen to its edges as the load increases between the points D and E. At a load level of ~340 pounds, the primary delamination reaches a length of almost half an inch. Thus, the primary delamination is of a progressive nature that causes considerable loss of the global specimen stiffness prior to final failure. When the load reaches 345 pounds, longitudinal compression and tension failures in the plies begin to develop. These longitudinal failures occur in the three upper and three lower plies close to the top and bottom of the specimen, respectively. Point F (350 pounds) marks failure of the specimen due to the loss of bearing capacity of the mid-span section.

The interior of the failed short RCC specimen obtained in the NASA experiments is shown in Fig. 4. The predicted primary and secondary delaminations can be seen, together with the failed middle section of the specimen. Note particularly that the locations, sizes and qualitative differences between the two delaminations were correctly predicted by the numerical simulation.

**Table 2 Mechanical properties of the RCC matrix**

Property	Value
Elastic modulus	0.80E6 psi
Shear modulus	3.25E5 psi
Poisson's ratio	0.23
Tensile strength	6.50E3 psi
Compressive strength	2.00E4 psi
Shear strength	3.40E3 psi
Tensile failure strain	0.02
Compressive failure strain	0.05
Shear failure strain	0.04

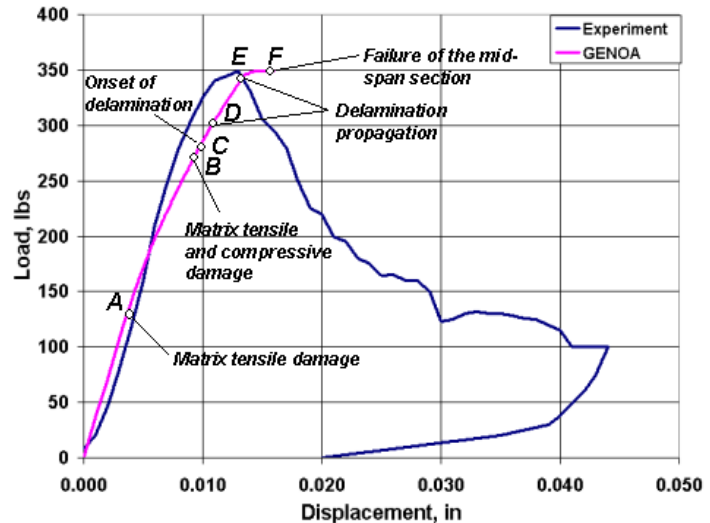


**Figure 3. Load-displacement response of the short RCC plate specimen.**

The inclined crack, which emanates from the broken top ply in Fig. 4, was not predicted in the GENOA analysis. This may be explained by the fact that this crack was likely to occur after the failure of the middle section of the specimen, and the unstable part of the load-displacement curve was not calculated in the present progressive failure analysis.

### B. Long Plate Specimen

The predicted load-displacement response of the long RCC plate specimen is shown versus the experimental data in Fig. 5. As in the previous case, points A through C on the predicted load-displacement curve indicate the onset of various types of damage in the specimen with the increase of the external load. At point A (~115 pounds), transverse matrix micro-cracking initiates at the center portion of bottom ply of the specimen. Also, at point A, the modified distortion energy criterion in Eq. 1 is violated at the center portion of bottom ply. When the applied load reaches 170 pounds (point B in Fig. 5), transverse tensile damage spreads upwards to plies 2-4. In addition, transverse compressive damage initiates in the top ply. All the mentioned types of damage, namely, transverse tensile and compressive damage, and damage due to violation of the modified energy criterion caused by the combination of various stress factors progressively grow between the loading points B and C. At the limit point C, when the load level reaches its maximum value of ~230 pounds, longitudinal compressive damage develops in the upper plies while longitudinal tensile damage initiates in the lower plies. This damage involves fiber breakage thus leading to failure of the specimen. In addition, some minor delamination damage develops in the lower and upper plies near the mid-span of the specimen as a result of excessive relative rotations between the adjacent plies.

The interior of the failed long RCC specimen, obtained in the NASA experiments, is shown in Fig. 6. Failure of the mid-span section, together with the minor delamination near the mid-span of the specimen, were correctly predicted by the analysis.

### V. Conclusion

A progressive failure analysis of two reinforced carbon-carbon plate specimens subject to three-point bending was carried out using the GENOA computer code. The analysis revealed significant qualitative differences in the response of the short and long plate specimens.

The short (one inch long) specimen exhibits primary and secondary delaminations. The primary delamination is of a progressive nature

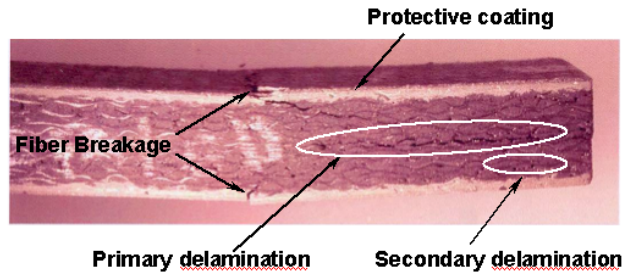


Figure 4. Failed short RCC plate specimen obtained in the NASA experiments.

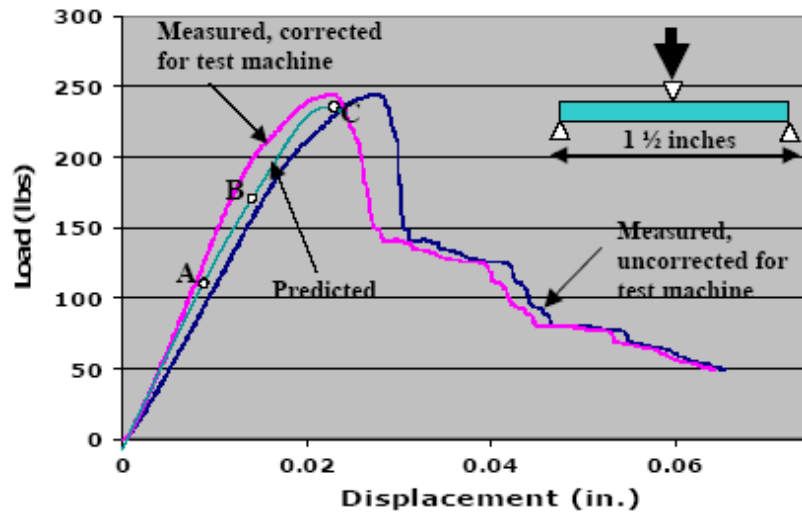


Figure 5. Load-displacement response of the long RCC plate



Figure 6. Failed long RCC plate specimen obtained in

that causes considerable loss of the global specimen stiffness prior to final failure. The long (one-and-a-half inch long) specimen shows only negligible delamination damage. Failure of both specimens occurs due to the loss of bearing capacity of the mid-span section. The predicted failure patterns, load-displacement response and limit loads for both of the specimens are in excellent agreement with the NASA test data.

The present study demonstrates that a proper choice of relative dimensions can effectively prevent catastrophic delamination failure of RCC composite plates.

### Acknowledgments

The first author would like to express his sincere gratitude to Dr. Dade Huang for all his valuable suggestions and encouragement during the work on this project.

### References

- <sup>1</sup>Anonymous, "Leading Edge Structural Subsystem Mechanical Design Allowables for Material With Improved Coating System," Loral-Vought Systems, Rept. 221RP00614, Oct. 1994.
- <sup>2</sup>Murthy, P. L. N., Chamis, C. C., "Integrated Composite Analyzer (ICAN), Users and Programmers Manual," NASA TP-2515, 1986.
- <sup>3</sup>Minnetyan, L., Chamis, C. C., and Murthy, P. L. N., "Structural Behavior of Composites with Progressive Fracture," *Journal of Reinforced Plastics and Composites*, Vol. 11, No. 4, 1992, pp. 413-442.
- <sup>4</sup>Huang, D., "Computational Simulation of Damage Propagation in Three-Dimensional Woven Composites," Ph.D. Dissertation, Civil Engineering Dept., Clarkson Univ., Clarkson, NY, 1997.
- <sup>5</sup>Farahmand, B., *Fracture Mechanics of Metals, Composites, Welds, and Bolted Joints. Application of LEFM, EPFM, and FMDM Theory*, Kluwer Academic Publishers, Boston, 2000, Chap. 8.
- <sup>6</sup>Chamis, C. C., "Failure Criteria for Filamentary Composites," *Composite Materials Testing and Design*, ASTM STP 460, American Society for Testing and Materials, Philadelphia, 1969, pp.336-351.